Available online at www.sciencedirect.com

ScienceDirect

Procedia Engineering 102 (2015) 1092 – 1103

Procedia Engineering

www.elsevier.com/locate/procedia

The 7th World Congress on Particle Technology (WCPT7)

Operation diagram of Circulating Fluidized Beds (CFBs)

H.L. Zhang[1], J. Degrève[1], R. Dewil[2] and J.Baeyens[3]*

[1] *KU Leuven, Dept. Chemical Engineering, De Croylaan 46, Heverlee, 3001, Belgium*
[2] *KU Leuven, Dept. Chemical Engineering, Process and Environm. Technol. Lab, Sint-Katelijne-Waver, 2860, Belgium;*
[3] *University of Warwick, School of Engineering, Coventry CV4 7AL, United Kingdom*

Abstract

CFBs are widely used in the chemical, mineral, environmental and energy process industries. Several authors stressed the need for a clear identification of the different operation regimes in the riser of a CFB, to ensure a better comprehension of the hydrodynamic context, and thus better define the operation and design parameters.. First approaches to develop a "work map" of the riser operation, were presented by e.g. Grace[1], Yerushalmi and Avidan[2], Bai *et al*.[3]. It was further developed by Chan *et al*.[4] and Mahmoudi *et al*.[5,6] for both Geldart A- and B-type powders, in terms of the operating gas velocity (U) and the solids circulation flux (G), which jointly delineate different regimes, called respectively Dilute Riser Flow (DRF), Core-Annulus Flow (CAF) (possibly with a bottom Turbulent Fluidized Bed, TFBB), and Dense Riser Upflow (DRU). For a given powder and its associated transport velocity, U_{TR}, the combination of U and G will determine the flow regime encountered. Experiments in CFB risers of 0.05 (2.5 m high), 0.1 and 0.15 m I.D. (both 6.5 m high), have demonstrated that common riser operations can be hampered by a specific (U,G) range where choking occurs. Angular sand, rounded sand, and spent FCC (all A-type powders) were used as bed material. Gas velocities were varied between 2 and 10 m/s, for solids circulation fluxes between 10 and 260 kg/m²s. Choking is understood as the phenomenon where a small change in gas or solids flow rate prompts a large change in the pressure drop and/or solids holdup during the gas-solid flow: the stable riser upflow regime is no longer maintained when G-values exceed a certain limit for a given gas velocity. Experimental results were empirically correlated, and proved to be about 30 % lower than predicted by the correlation of Bi and Fan[7], but largely exceeding other predictions. Introducing the findings into the available operation diagram [5,6], adds a region where stable riser operation is impossible. The adapted diagram enables CFB designers to better delineate the operating characteristics.

Keywords: Circulating Fluidized Beds; Choking Velocity; Operations; Solids Circulation Flux; Gas Velocity

Selection and peer-review under responsibility of Chinese Society of Particuology, Institute of Process Engineering, Chinese Academy of Sciences (CAS)

* Corresponding author. Tel.: +32 16 53 28 34;
E-mail address: baeyens.j@gmail.com

Selection and peer-review under responsibility of Chinese Society of Particuology, Institute of Process Engineering, Chinese Academy of Sciences (CAS)
doi:10.1016/j.proeng.2015.01.232

Nomenclature

Ar	Archimedes number, [-]
D	riser diameter, [m]
d_p	particle size, [μm]
F_{45}	fraction of particles which diameter is less than 45μm
G	solids circulation flux, [kg/m^{2}s]
g	gravitational constant, [m/s^2]
H	height of the riser, [m]
Re_t	Reynolds number at terminal velocity, [-]
Re_{tf}	Reynolds number at the onset of turbulent fluidization, [-]
Re_{TR}	Reynolds number at U_{TR}, [-]
U	superficial gas velocity, [m/s]
U_{mb}	minimum bubbling velocity, [m/s]
U_{mf}	minimum fluidization velocity, [m/s]
U_{tf}	gas velocity at the onset of turbulent fluidization, [m/s]
U_{TR}	transport velocity of particles, [m/s]
U_t	terminal velocity of particles, [m/s]
$U_{trans.}$	regime transition velocity, [m/s]
U_{Ch}	choking velocity, [m/s]
U_{salt}	saltation velocity, [m/s]
U_{ms}	velocity at onset of slugging, [m/s]
U_{slip}	slip velocity of the particles, [m/s]
$\overline{v_p}$	average particle velocity, [m/s]
μ_g	viscosity of gas
μ_{air}	viscosity of air
ε	CFB voidage, [-]
ε_b	voidage of the turbulent fluidization bottom bed, [-]
ε_{Ch}	voidage of the choking bed, [-]
ρ_p,ρ_b,ρ_g	particle, bulk and gas density, respectively, [kg/m^3]

1. INTRODUCTION

CFBs are widely used in the chemical, mineral, environmental and energy process industries. Several authors stressed the need for a clear identification of the different operation regimes in the riser of a CFB, to ensure a better comprehension of the hydrodynamic context, and better define the design and operation parameters. First approaches to develop a "work map" of the riser operation, were presented by e.g. Grace[1], Yerushalmi and Avidan[2], Bai *et al.*[3]. It was further developed by Chan *et al*. [4] and Mahmoudi *et al*. [5,6] for both Geldart A- and B-type powders: the operating gas velocity (U) and the solids circulation flux (G) jointly delineate different regimes, called respectively Dilute Riser Flow (DRF), Core-Annulus Flow (CAF) (possibly with a Turbulent Fluidized Bed at the Bottom of the riser, TFBB), and Dense Riser Upflow (DRU). For a given powder and its associated transport velocity, U_{TR}, the combination of U and G will determine the flow regime encountered.

The dominant parameter in fluidisation is the gas velocity. In CFBs and pneumatic conveyors, the solids loading in general, and solids circulation rate in the CFB are also important. Avidan and Yerushalmi [8] and Yerushalmi and Crankfurt [9] presented different operating regimes in terms of the system voidage and the slip velocity, defined by Equation (1), and relating the average particle velocity, $\overline{v_p}$, with the interstitial gas velocity U/ε.

$$U_{slip} = \frac{U}{\varepsilon} - \overline{v_p} \quad (1)$$

Figure 1 illustrates the different operation modes of powder gas systems, with representative values of the major characteristic parameters.

A few selected empirical equations to determine the fluidization velocity at the transition of subsequent operation regimes are presented in Table 1 to predict the regime transition velocities, U_{trans}. For pneumatic conveying applications, additional critical velocities are the choking velocity (U_{Ch}) for vertical transport, and the saltation velocity (U_{salt}) for horizontal transport.

Table 1: Prediction of transition velocities

U_{trans}	Equations	Ref.
U_{mb}	$U_{mb} = \frac{2.07 d_p \rho_g^{0.06}}{\mu_g^{0.347}} \exp(0.716 F_{45})$, F_{45}: fine fraction less than 45μm	[10]
U_{mf}	$Ar = 1823 Re_{mf}^{1.07} + 21.27 Re_{mf}^2$	[11]
U_{tf}	$Re_{tf} = 1.24 Ar^{0.45}, for\ 2 < Ar < 10^8$	[12]
U_{TR}	$Re_{TR} = 3.23 + 0.23 Ar$	[13]
U_{Ch}	$\frac{2gD(\varepsilon_{Ch}^{-4.7} - 1)}{(U_{Ch} - U_t)} = 0.00872 \rho_g^{0.77}$	[14]
U_{salt}	$U_{salt} = 4.43 \sqrt{\frac{\rho_p - \rho_g}{\rho_g} d_p}$	[15]
U_{ms}	$U_{ms} = U_{mf} + 0.07\sqrt{gD}$, D: diameter of the bubbling fluidized bed	[16]

A CFB-riser operates at moderate to high slip velocities and ε >> 0.9. Chang and Louge [17] indicate that the flow in the riser can be isolated from the other parts of the CFB if G is controlled. The properties in the return loop (standpipe) do influence the nature of flow in the riser if G is not properly controlled [18]. As far as the operating gas velocity (U) is concerned, a stable CFB-operation requires external solids circulation and is only possible at velocities in excess of the transport velocity (U_{TR}). Combining own experimental results and literature data for powders of Ar ≤ 500, Zhang [13] developed Eqn. (2) for U_{TR}. It is however recommended to operate the riser at a velocity in excess of U_{TR}, since empirical correlations are expected to be within a 10% accuracy for different powder systems.

$$U_{TR} = \left(\frac{\mu_{air}}{\rho_{air} d_p}\right)(3.23 + 0.23 Ar) \quad (2)$$

Some of the previous studies observed a bed at the bottom and a dilute phase at the top of the riser [19-23]. The axial solids hold-up profile has an inflection point, and this profile is referred to as S-profile. The bed progressively becomes deeper under increasing higher solid flux [24-28]. Other researchers however indicate that an exponential profile for solids hold-up exists with no dense bed but with an acceleration zone at the bottom of the riser, considered to be characteristic of other regimes such as core-annulus flow without bed, dilute transport and/or dense core flow [12,21,28-30].

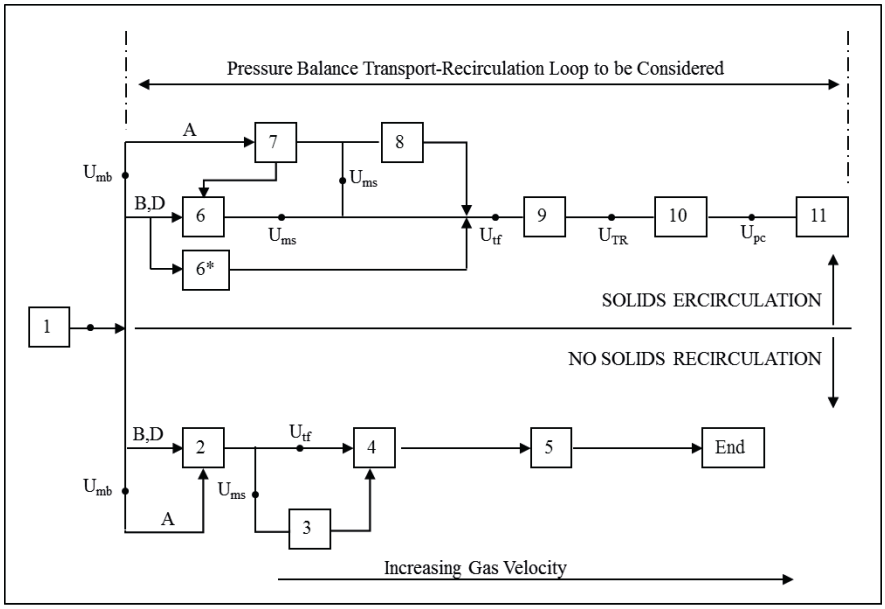

1. Packed Bed
2. Bubbling Fluidized Bed (A, B, D: Powders of Geldart Classes)
3. Slugging Bed
4. Turbulent Fluidized Bed
5. Elutriation/Carry-over
6. Bubbling transport
6*. Bubbling Fluidized Bed with an internal draft tube
7. Bubble-free dense transport
8. Slugging dense transport
9. Turbulent dense transport
10. CFB
11. Homogeneous Dilute Phase Transport

Characteristcs of various fluidization regimes

U_{mf}	U_{mb}	U_{ms}	U_{tf}	U_{TR}	U_{pc}
1	2, 6, 7, 6*	3, 8	4, 9	10	11

Powder	Parameter	Regime			
		2, 6	4, 9	10	11
A	U (m/s)	~0.01-~0.5	0.5-~1.5	>1.5	>1.5
	ε	0.4-0.65	0.65-0.8	0.8-0.98[f(G)]	>0.9 dense conveying ~1 dilute conveying
B	U (m/s)	0.05->1[f(d_p)]	Only achieved at smaller d_p-range of B powder	>1.5	>3
	ε	0.4-0.5		0.8-0.98[f(G)]	>0.9 dense conveying ~1 dilute conveying

Figure 1: Operation modes of powder-gas systems

From the extensive literature survey, and own experiments, four distinct solids hydrodynamics modes are confirmed in a CFB operation. The 4 distinct regimes are:

Dilute Riser Flow (DRF), where the solids are predominantly moving upwards with negligible downward flow. The axial voidage profile is typically exponential with one acceleration zone at the bottom of the riser, near the

solids return entry. The velocity of the solids can be predicted by the Geldart equation [31] using the terminal particle velocity as slip velocity:

$$\overline{v_p} = \frac{U}{\varepsilon} - U_t \quad (3)$$

The particle velocity has also been expressed by an alternative Equation (4), introducing the slip factor, φ, resulting in:

$$\overline{v_p} = \frac{U}{\varepsilon\varphi} \quad (4)$$

In DRF-regime, the slip factor, φ has a value between 1 [30] and 1.2 [4].

In **Core-annulus Flow (CAF),** the solids motion is an upward core flow and downward flow in the annulus. The voidage is typically exponential along the axial direction and the solids velocity can be predicted by Equation (4), with φ values close to 2 [32, 33]. Under specific combinations of U and G, **Core-annulus Flow (CAF)** with **Turbulent Fluidised Bottom Bed (TFBB)** occurs. The axial voidage profile is of typical S-nature, due to the appearance of a Turbulent Fluidised Bottom Bed (TFBB). Chan et al. [27] demonstrated that the residence time for solids in TFBB alone can range from 10 to 20s. The voidage of the TFBB ranges from 0.7 to 0.9 and can be predicted by the empirical equation (5) [34]. The characteristics of the CAF region above the TFBB are similar to the above sole CAF flow, as described before.

$$\varepsilon_b = \frac{U+1}{U+2} \quad (5)$$

Chan et al. [4] found that the **Dense Riser Upflow (DRU)** has almost similar characteristics to DRF, the main difference being that the φ values are fractionally higher, ranging between 1.2 and 1.6 with an average of 1.3.

These various hydrodynamics regimes are also have a distinct bed voidage ranging from approximately 0.98 in dilute flow (DRF); 0.7-0.9 in a bottom fluidised bed (TFBB), 0.97-0.99 in core-annulus mode (CAF), to ~ 0.9 in dense riser upflow DRU [35-37]. These voidages can be estimated by the method of Chan et al. [4], with U, G and ρ_p as controlling parameters.

The "work map" of the CFB, as developed by Mahmoudi *et al.* [5,6] for both A and B type powders, is illustrated in Figure 2, A-B, with the demarcation lines between the regimes as shown in the figures to separate the different experimentally observed regimes, fitted by appropriate equations.

(a) II/III: $G = 10 + (U - U_{TR})^{1.8}$ (6)

(b) III/IV: $G = 20 + (U - U_{TR})^{2}$ (7)

(c) IV/V: $G = 60 + 15(U - U_{TR})^{0.5}$ (8)

The velocity range close to U_{TR} is not indicated since some data points can be considered in a riser flow mode, whereas other data points are still in a turbulent fluidised bed mode. It is therefore recommended to respect a velocity margin of about 0.2 m s $^{-1}$ above U_{TR}.

The range of operating U and G for the known commercial risers was reviewed by Mahmoudi *et al*. [38] and by Van de Velden *et al*. [19,39,40], with reported CAF operation in the range of U-U_{TR} = 0.5 to 5 m s $^{-1}$ and G-values of 10 to about 80 kg m^{-2}s^{-1}. CFB operations in DRU-mode are reported for U-U_{TR} values exceeding about 8 m s^{-1} and G-values between 150 and 1200 kg m^{-2}s^{-1}. These reported modes are in good agreement with the proposed operation diagram of Figures 2.

Common riser operations can however be hampered in a specific (U,G) range where choking occurs, being understood as the phenomenon where a small change in gas or solids flow rate prompts a significant change in the pressure drop and/or solids holdup: the stable riser upflow regime is no longer maintained when G-values exceed a certain limit for a low to moderate gas velocity. Considerable efforts have been made in probing choking in CFBs, and several empirical equations have been proposed, as summarized in Table 2.

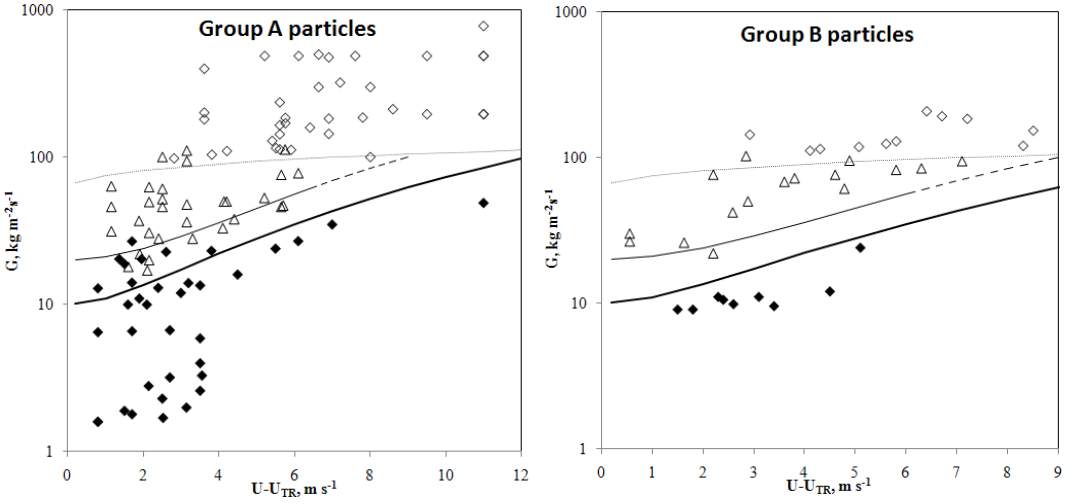

Figure.2-A-B : The different operating regimes for group A and B powders [5,6].

◆DRF
△CAF with/without TFBB
◇DRU
Equation 6
Equation 7
Equation 8
– – – Range of operating conditions where CAF mode is no longer reported and only DRF and DRU prevail

Table 2: Literature correlations to predict choking velocities, U_{Ch}

Authors	Equations	
[41]	$U_{Ch} = 32.3\frac{G}{\rho_p} + 0.97U_t$	(9)
[42]	$U_{Ch} = 10.74U_t\left(\frac{G}{\rho_p}\right)^{0.227}$	(10)
[43]	$\frac{U_{Ch}}{\sqrt{gd_p}} = 32Re_t^{-0.06}\left(\frac{G}{\rho_g U_{Ch}}\right)^{0.28}$	(11)
[7]	$\frac{U_{Ch}}{\sqrt{gd_p}} = 21.6\left(\frac{G}{\rho_g U_{Ch}}\right)^{0.542} Ar^{0.105}$	(12)

The objective of the present research hence considered (i) the delineation of the choking phenomenon in different riser geometries, and using different A-type powders; (ii) the comparison of experimental results with the empirical predictions of the equations of Table 2, and finally (iii) to adapt the proposed operation diagram of Mahmoudi *et al.* [5,6] to include the (U,G) region subject to choking.

2. MATERIALS AND METHODS

The typical layout is illustrated in Figure 3.

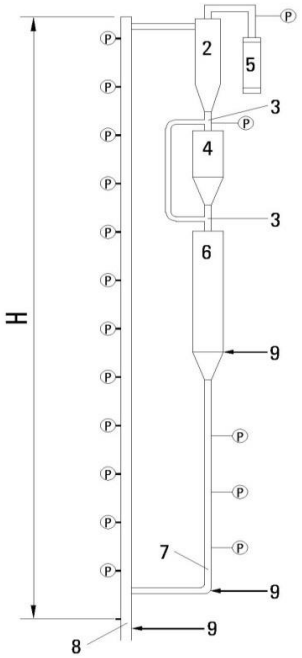

Figure 3. The lab-scale CFBs with 1. Riser; 2. Cyclone; 3. Diverter valve; 4. Measuring bed; 5. Bag filter; 6. Slow bed; 7. L-valve; 8. Metal gauge distributor; 9. Air from Roots blower; P. Pressure tapping

Three risers, built in transparent polyethylene to enable a visual observation of the solids flow, were used: 0.05, 0.1 and 0.15 m I.D., with respective heights of 2.5, 6.5 and 6.5 m. The exits of the risers are sharp (90°). Filtered air from a compressor is fed both to the riser through a metal gauge distributor plate, and to the recycle solids L-valve. The air velocities are determined from rotameter readings. The riser exit air passes a high efficiency Stairmand cyclone, followed by a fabric filter. Filter dust is periodically returned to the unit. The cyclone apex discharges the collected solids in the recycle loop, comprising a "slow" fluidized bed, and a by-pass measuring bed. The slow bed, constructed as a fluidized bed with a diameter in excess of the other parts of the loop, creates the required pressure build-up to compensate the pressure drop of riser and cyclone: the slow bed has a diameter of 0.15 m (0.05 m I.D. riser), and 0.29 m I.D. for both other risers. The height of the slow bed (fluidized at ~3 x U_{mf}) is between 0.4 and 0.9 m. The fluidizing air from the slow bed is vented to the fabric filter for dust removal. Solids from the cyclone discharge are periodically diverted for a given time to a measuring bed, where the solids circulation flux is measured from the collected volume (for a known Δt) and bulk density of solids, considered as the bulk density of their fixed bed. Measured solids are returned into the rig whilst in operation. The L-valves have respective diameters of 0.025 m (small riser) and 0.05 m (both larger risers). The L-valve enters the column ~ 10 cm above the distributor. Pressure tappings (provided with glass wool plug to prevent ingress of powder into the measuring lines) are installed every 0.5 m up the riser height. ΔPs were measured by both water manometers, and by solid state pressure transducer in the 0.1 and 0.15m I.D. rigs (with A/D converter and PC data logging). Pressure gradients along the height of the riser were measured. Powders used in the experiments are listed in Table 3, with corresponding relevant characteristics. Average particle sizes were measured by laser diffraction analysis (Malvern). 90 % of the particle size distribution was situated between the range specified in Table 3. Bulk and absolute densities were separately measured. The terminal velocity was calculated by the Geldart method [31].

Table 3. Powders used in the different rigs

Powder	d_p (μm)	ρ_p (kg/m³)	90 % range (μm)	Ar	U_t (m/s)	U_{TR} (m/s)	Riser I.D. (m)
Rounded sand	74	2260	45-90	33	0.44	2.20	0.05
Angular sand	72	2660	35-95	36	0.41	1.73	0.1
Spent FCC	70	1630	45-100	20	0.24	1.69	0.1
Rounded sand	84	2260	35-110	48	0.46	2.56	0.1
Angular sand	98	2660	60-130	98	0.77	3.67	0.15

For a given solids flux, G, the gas flow was progressively and gradually reduced from ~ 10 m/s. The initial increase in ΔP over the bottom section of the riser corresponds with forming a turbulent fluidized bed at the riser bottom (TFBB), however with continued solids elutriation. At increased G, or reduced U, it is followed by the collapse of the solids into a slugging state, with its characteristic ΔP-fluctuation frequency of 0.7 - 1 Hz [44]. A further decrease of the gas velocity at the given G leads to the formation of a fixed bed, without further upward solids transport. At the given G-value of slugging, the corresponding gas velocity was selected as choking velocity, U_{Ch}, in the present study. Gas velocities were varied between 2 and 10 m/s, for solids circulation fluxes between 10 and 260 kg/m²s.

3. RESULTS AND DISCUSSION

Characteristics of powders and the dimensions of the risers they were tested in, are given in Table 3. Observed choking conditions, are presented in Figure 4 with corresponding choking velocities, U_{Ch}, at given solids circulation flux (G). Results illustrate that the particle size has a significant influence at higher values of G; and that the choking velocity increases when G increases. No pronounced effect of the riser I.D. (0.05-0.10 I.D. for sand of 70 -84 μm) was noticed.

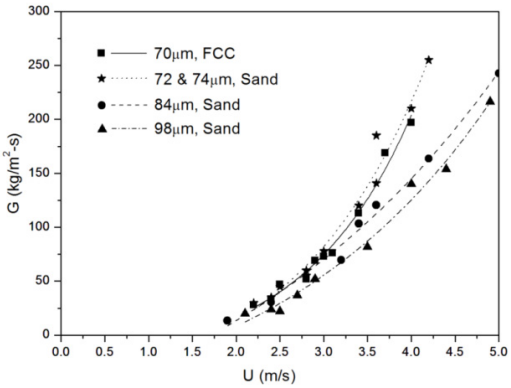

Figure 4. Experimental choking solids circulation flux, G, versus choking velocity U_{Ch} (left of data points: choking; right: stable circulating bed). Characteristics of powders and rigs used are given in Table 3.

The comparison of experimental data and literature predictions (Table 2) is illustrated in Figure 5 for the 84μm rounded sand. For all powders, Leung *et al*. [41] and Matsen [42] underestimate U_{Ch}. The Yousfi and Gau [43] prediction is fair at lower U- and/or G-values. This is also the case when using the Bi and Fan [7] equation: a fair prediction at low U and/or G is followed by an overestimation at increasing U-values, although the trend of the predictions is fairly parallel with the experimental measurements. This parallelism was further investigated in Figure 6 for all powders.

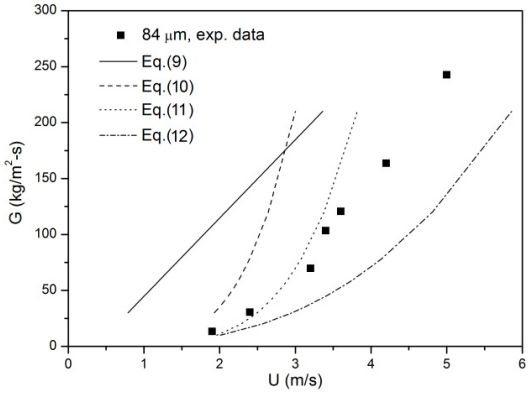

Figure 5. Comparison of experimental data for 84μm rounded sand, with predictions by equations (Table 2)

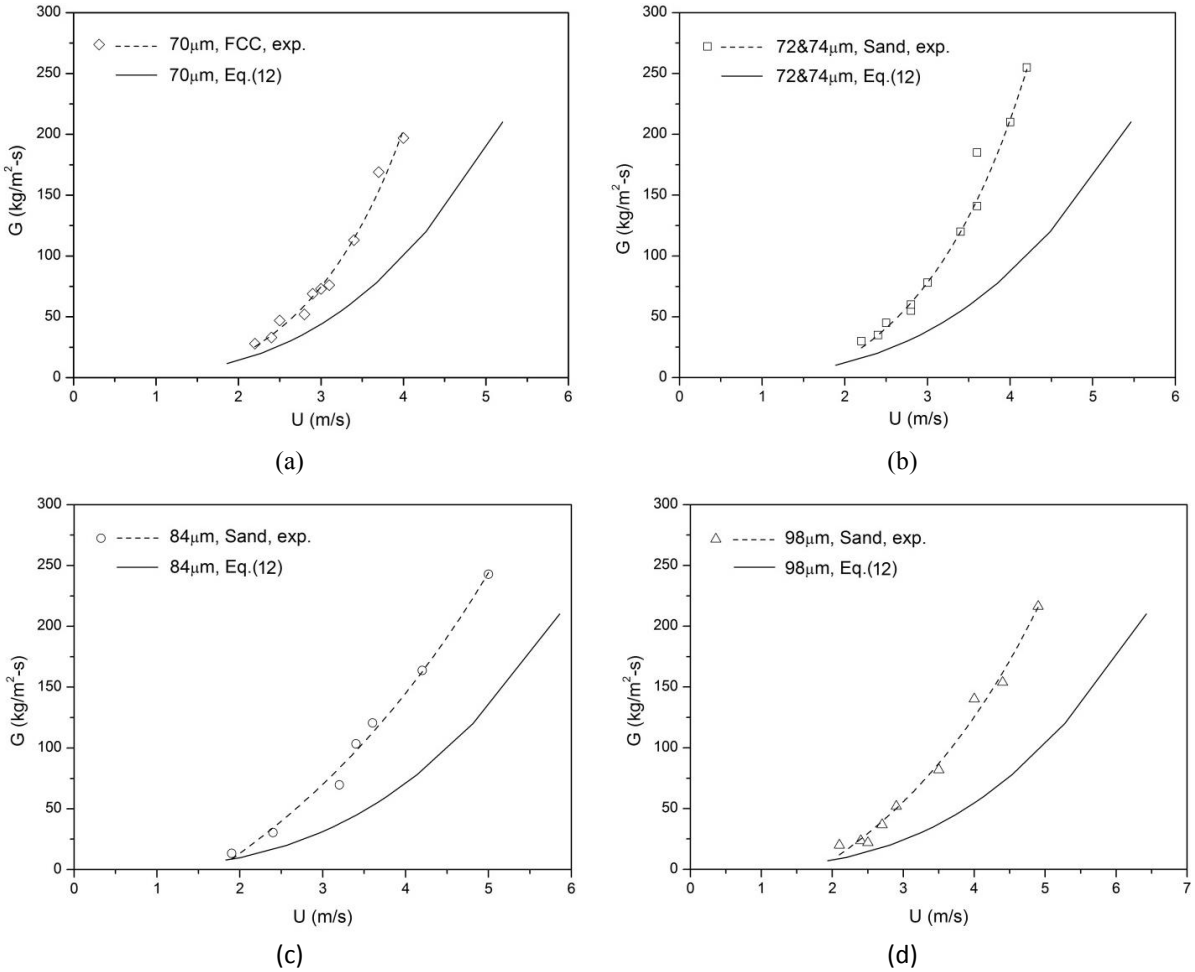

Figure 6. Comparison of the Eq.(4)-predicted (G_{Ch}-U_{Ch}) values with experimental data

In view of the overestimation by Eq. (12), especially at $U \geq 2$m/s, experimental results were correlated with a slightly modified Bi and Fan-equation, the only difference being the empirical coefficient, reduced from 21.6 to 14.6 in the case of the present study. The resulting equation is given as:

$$\frac{U_{Ch}}{\sqrt{g d_p}} = 14.6 \left(\frac{G}{\rho_g U_{Ch}}\right)^{0.542} \cdot Ar^{0.105} \qquad (13)$$

The comparison of all experimental data, with Eq. (13) is illustrated in Figure 7-A.

To compare the predictive value of Eq. (13) with scarce literature data on choking conditions, Figure 7-B was developed. Literature data are scarce outside the experimental data that lead to the establishment of the empirical equations of Table 2. Additional data were extracted from graphs given in papers by Du and Fan [45], Du *et al*.[46], and Bai *et al*. [47]. A comparison of the extracted data and the prediction of Eq. (13) is illustrated in Figure 7-B. The prediction is seen to be fair, even beyond the range of our experimental G-values.

Having established a correlation for U_{Ch} in terms of gas and solids properties, the "work" diagram of Mahmoudi *et al*. [5,6], can be adapted, as illustrated in Figure 8, where it can be seen that the occurring choking regime is specifically important at high values of G, and/or low values of (U-U_{TR}). An inaccuracy of 0.2m/s was indicated with respect of U_{TR} predictions from Eq.(2).

Both U_{TR} and the delineation curve separating zone I_B from zone V should be calculated for the specific particle-gas system under scrutiny. For Zone V (DRU) operation, U-values commonly exceed 10 m/s with G-values in excess of 800 kg/m²s. This operation is certainly beyond the U,G-region where choking is likely to occur. Choking should be considered in the transition regime between Zones IV and V whenever lower excess gas velocities are selected.

The resulting operation diagram of a CFB-riser better delineates operating characteristics. Choking does not affect the CAF operation mode, but delays a stable DRU-mode to higher velocities than predicted by U_{TR}. The use of equations from Table 2 will either over predict (Eqn. 12) or underestimate (Eq. 9-11) the excess gas velocity needed to avoid choking.

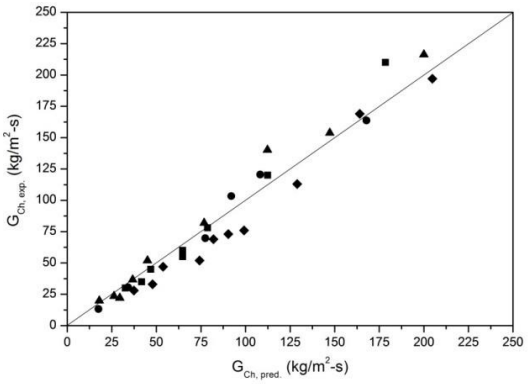

A. Comparison of the Eq.(13)-predicted $G_{Ch,\,pre.}$ values with experimental data $G_{Ch,exp.}$ for

(a) ◆ 70μm FCC; (b) ■ 72 and 74 μm Sand;

(c) ● 84μm Sand; (d) ▲ 98μm Sand

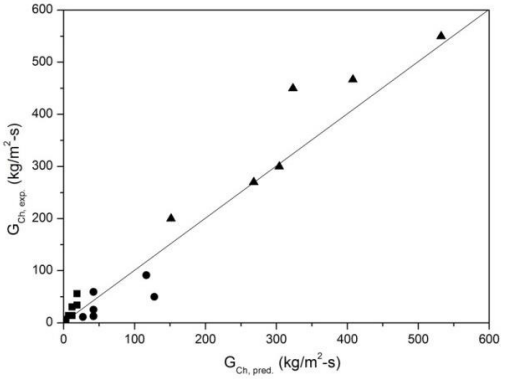

B. Comparison of the Eq.(13)-predicted $G_{Ch,\,pre.}$ values with experimental data $G_{Ch,exp.}$ from references of

(a) ■ Du and Fan[45]; (b) ● Du *et al*.[46];

(c) ▲ Bai *et al*.[47].

Figure 7 Comparison of the Eq.(13)-predicted $G_{Ch,\,pre.}$ values with experimental data $G_{Ch,exp.}$

4. CONCLUSIONS

The choking velocity was measured for different powders in different riser geometries. Equation (13) predicts U_{Ch} for a specific gas-solid system. The existence of a distinct choking region in the operation of the riser, implies that a previously presented operation diagram is extended with an additional region, especially at low values of (U - U_{TR}) and higher values of G, where choking will prevent a stable riser operation, as presented in Figure 8.

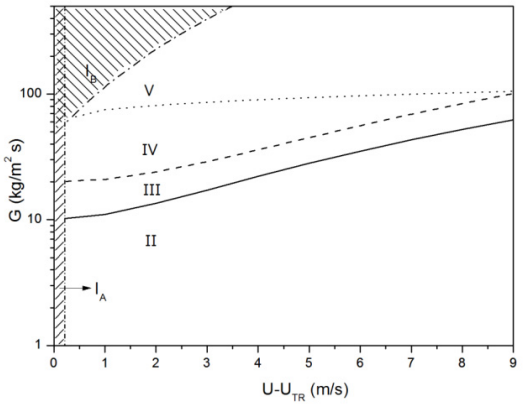

Figure 8. Operation of a CFB riser, as G versus U-U_{TR} (adapted from[5.6])

Zone I_A: Zone I: Transition zone and/or inaccuracy in U_{TR} prediction; Zone I_B: Zone of choking; Zone II: dilute riser flow (DRF); Zone III: core-annulus flow (CAF) only; Zone IV: CAF with turbulent fluidized bed at the bottom (TFBB) of the riser; Zone V: dense riser up-flow (DRU).

——— transition DRF - CAF: $G = 10 + (U - U_{TR})^{1.8}$

– – – – – transition CAF - CAF with TFBB: $G = 20 + (U - U_{TR})^{2}$

····· transition CAF with TFBB - DRU: $G = 60 + 15\,(U - U_{TR})^{0.5}$

–·–·–·– 84μm Sand: Eq.(13) predicted

References

[1] Grace, J.R., 1990. High velocity fluidized bed reactors. Chemical Engineering Science, 45, 1953-1966.

[2] Yerushalmi, J. and Avidan, A., 1985. High velocity fluidization. In: Fluidization, 2nd ed., Davidson, J.F., Clift, R. and Harrison, D. (Eds.), Academic Press: New York, 225-289.

[3] Bai, D., Shibuya, E., Masuda, Y., Nishio, K., Nakagawa, N. and Kato, K., 1995. Distinction between upward and downward flows in circulating fluidized beds. Powder Technology 84, 75-81.

[4] Chan, W., Seville, J.P.K., Parker, D., Baeyens, J. 2010. Particle velocities and their residence time distribution in the riser of a CFB. Powder Technology 203(2), 187-197.

[5] Mahmoudi, S., Baeyens, J., Seville, J.P.K., 2011. The solids flow in the CFB-riser quantified by single radioactive particle tracking. Powder Technology 211 (11), 135-143.

[6] Mahmoudi, S., Chan, C.W., Brems, A., Seville, J.P.K., Baeyens, J., 2012. Solids flow diagram of a CFB riser using Geldart B-type powders. Particuology 10(1), 51-61.

[7] Bi, H.T. and Fan, L.S., 1991. Regime transitions in gas-solid circulating fluidized beds. AIChE. Annual Meeting. AIChE, Los Angeles 17-22

[8] Avidan, A.A. and Yerushalmi, J., Bed expansion in high velocity fluidization, Powder Technology, 32 (1982), p. 223-232

[9] Yerushalmi, J. and Crankfurt, N.T., Further studies of the regimes of fluidization, Powder Technology, 24 (1979), p. 187-205

[10] Abrahamsen, A.R., Geldart, D., 1980. Behavior of gas-fluidized beds of fine powders. Part I: homogeneous expansion. Powder Technology 26,35–46.

[11] Wu, S.Y. and Baeyens, J., Effect of operating temperature on minimum fluidization velocity, Powder Technology, 67 (2), (1991), p. 217-220

[12] Bi, H.T., Grace, J.R., Flow regime diagrams for gas-solid fluidization and upward transport, International Journal Multiphase Flow 21 (1995), pp. 1229-1236.

[13] Zhang, H.L., Powder circulation systems for heat storage. PhD-dissertation K.U.Leuven, 2014. to be published

[14] Punwani, D.V., Modi, M.V. and Tarman, P.B., A generalized correlation for estimating choking velocity in vertical solids transport. Paper presented at the International Powder Bulk Solids Handling and Processing Conference, Chicago, Illinois (1976)

[15] Brook, N., Fluid transport of coarse solids, Mineral Science Technology, 5 (1985), p. 197-217

[16] Baeyens, J., and Geldart, D., 1974. An investigation into slugging fluidized beds. Chemical Engineering Science 29(1), 255-265

[17] Chang, H., and Louge, M., Fluid dynamic similarity of circulating fluidized beds, Powder Technology, 70 (1992), p. 259-270

[18] Schnitzlein, M. G., and Weinstein, H.. Design parameters determining solid hold-up in fast fluidized bed system. In: Proceedings of the second international conference on circulating fluidized beds, Basu, P. and J. F. and Large, J.F., (Eds), Compiegne, France. Oxford: Pergamon Press, (1988), p. 205-211

[19] Van de Velden, M., Baeyens, J., Dougan, B. and McMurdo, A., Investigation of operational parameters for an industrial CFB combustor of coal, biomass and sludge, China Particuology, 5 (2007) p. 247-254

[20] Li, J., Tung, Y. and Kwauk, M., Axial voidage profiles of fast fluidized beds in different operating regions, In: Circulating Fluidized Bed Technology II, Basu, P. and Large, J.F. (Eds.), Pergamon, (1988), p. 193–203

[21] Kato, K.H., Shibasaki, H., Tamura, K., Arita, S., Wang, C. and Takarada, T., Particle hold-up in a fast fluidized bed, J.Chem.Eng.Japan, 22 (1989), pp. 130-136
[22] Mori, S., Kato, K., Kobayashi, E., Liu, D., Hasatani, M., Matsuda, H., Hattori, M., Hirama, T. and Takeuchi, H., Effect of apparatus design on hydrodynamics of circulating fluidized-bed, AIChE Symp. Ser. 289, 88 (1992) p. 17–25
[23] Rhodes, M.J., Sollaart, M. and Wang, X.S., Flow structure in a fast fluid bed, Powder Technology, 99 (1998), p. 194-200
[24] Malcus, S., Cruz, E., Rowe, C. and Pugsley, T.S., Radial solid mass profiles in a high-suspension density circulating fluidized bed, Powder Technology, 125 (2002), p. 5-9
[25] Karri, S.B.R. and Knowlton T.M., Wall solids upflow and downflow regimes in risers for Group A solids., In: Circulating Fluidized Bed Technology VII, Grace, J.R., Zhu, J. and de Lasa, H. (Eds), CSChE, Ottawa, Canada (2002), p. 310-316
[26] Manyele, S.V., Khayat, R.E. and Zhu, J., Investigation of the hydrodynamics of a high-flux CFB riser using chaos analysis of pressure fluctuations, Chemical Engineering and Technology, 25 (2002), p. 801-810
[27] Chan, C.W., Seville, J., Yang, Z. and Baeyens, J., Particle motion in the CFB riser with special emphasis on PEPT-imaging of the bottom section, Powder Technology, 196 (2009), p. 318-325
[28] Bai, D.-R., Jin, Y., Yu, Z.-Q. and Zhu, J.-X. The axial distribution of the cross-sectionally averaged voidage in fast fluidized beds, Powder Technology, 71 (1992), p.51–58
[29] Rhodes, M.J. and Geldart, D., The upward flow of gas-solid suspensions: Part 1. A model for the circulating fluidized bed incorporating dual level entry into the riser, Chem. Eng. Res. Des. 67 (1989), p. 20–29
[30] Hartge, E.-U., Rensner, D. and Werther, J., Solids concentration and velocity patterns in circulating fluidized beds, In: Circulating Fluidized Bed Technology II, Basu, P. and Large, J.F. (Eds.), Pergamon, (1988), p. 165–180
[31] Geldart, D., Particle entrainment and carry-over. In: Gas Fluidization Technology, Geldart, D. (Ed.). Wiley, New York, (1986) p. 123–153
[32] Matsen, J.M., Some characteristics of large solids circulation systems, In: Fluidization Technology, Keairns D.L. (Ed), Vol. 2, Hemisphere, (1976), p. 135
[33] Ouyang, S. and Potter, O.E., Consistency of Circulating Fluidized Bed Experimental Data, Ind. Eng. Chem. Res., 32 (1993), p. 1041-1045
[34] King, D., Estimation of dense bed voidage in fast and slow fludized beds of FCC catalyst, In: Fluidization VI, Grace, J.R. and Bergougnou, M.A. (Eds.), Engineering Foundation, New York, (1989), p. 1-8
[35] Smolders, K. and Baeyens, J., The transport disengaging height in fluidised bed. Powder Handling and Processing, 10 (1998), p. 27-36
[36] Smolders, K. and Baeyens, J, Gas fluidized bed operating at high velocities: a critical review of occurring regimes, Powder Technology, 119 (2001), p. 269-291
[37] Smolders, K. and Baeyens, J, Hydrodynamic modelling of the axial density profile in the riser of a low density CFB, Canadian Journal of Chemical Engineering, 79 (2001), p. 422-429
[38]Mahmoudi, S., Seville, J.P.K. and Baeyens, J., The residence time distribution and mixing of the gas phase in the riser of a circulating fluidized bed, Powder Technology, 203 (2), (2010), p. 322-330
[39] Van de Velden, M., Baeyens, J., Seville, J.P.K., Fan, X. The solids flow in the riser of a CFB viewed by Positron Emission Particle Tracking (PEPT), Powder Technology, 183, (2008), p. 290-296
[40]Van de Velden, M., Baeyens, J. and Smolders, K., Solids mixing in the riser of a circulating fluidized bed, Chemical Engineering Science, 62 (2007), p. 2139-2153
[41] Leung, L.S., Wiles, R.J. and Nicklin, D.J., 1971. Correlation for predicting choking flow rate in vertical pneumatic conveying. Industrial and Engineering Chemistry Process Design and Development, 10, 183-189.
[42] Matsen, J.M., 1982. Mechanisms of choking and entrainment. Powder Technology, 32, 21-33.
[43] Yousfi, Y., Gau, G., 1974. Aérodynamique de l'écoulement vertical de suspensions concentrées gaz-solides-I. Régimes d'écoulement et stabilité aérodynamique, Chemical Engineering Science, 29(9), 1939-1946.
[44] Baeyens, J. and Geldart, D., 1974, An investigation into slugging fluidized beds, Chem Eng Sci, 29: 255–265.
[45]Du, B. and Fan, L.S. 2004. Characteristics of choking behavior in circulating fluidized beds for Group B particles. Industrial Engineering Chemistry and Research 43, 5507-5520.
[46] Du, B., Warsito, W. and Fan, L.S. 2006. Imaging the choking transition in gas-solid risers using electrical capacitance tomography. Industrial Engineering Chemistry and Research 45, 5384-5395.
[47] Bai, D., Issangya, A.S. and Grace, J.R., 1998. A novel method for determination of choking velocities. Powder Teechnology 97, 59-62.